

Interactive comment on “Opposite Long-term Trends in Aerosols between Lower and Higher Altitudes: A Testimony to the Aerosol-PBL Feedback” by Zipeng Dong et al.

Zipeng Dong et al.

dzp2003@126.com

Received and published: 24 April 2017

Response to Anonymous Referee 2

We thank the referee for carefully reviewing our manuscript and providing suggestions to improve the clarity and quality of the paper.

1) For a reader who is not familiar with the aerosol-PBL feedback, maybe it is difficult to directly link the two points. The feedback scheme has been already well-established in previous studies, especially modeling works. The key point of this paper is to show how this process is important for specific regions and different part of China from a perspective of long-term trend. It will be better that the authors give more descriptions

C1

on the aerosol-PBL feedback in the introduction part based on existing studies. In the introduction part, it also could be directly pointed out that the aerosol-PBL feedback will cause enhanced lower PBL pollution and decreased upper PBL pollution, as that showing in Fig.1b of Ding et al. (2016).

We have added the following description of the mechanism behind the aerosol-PBL feedback in the introduction:

“Through scattering and absorption of solar radiation, atmospheric aerosols reduce net surface shortwave radiation (SSR) and thus induce surface cooling. The decreased net SSR reduces sensible heat fluxes (Zhang et al., 2008), which leads to weakened surface buoyancy fluxes (Tesfaye et al., 2014). Moreover, black carbon aerosols absorb solar radiation in the visible wavelengths and consequently warm up and stabilize the atmosphere. The changes in atmospheric radiative heating rate and atmospheric stability depend on the vertical distribution of aerosols (Gonçalves et al., 2015). If the absorbing aerosols are confined to the PBL, they may incur or strengthen a temperature inversion below the entrainment zone, leading to the suppression of vertical motions and to a shallower PBL (Barbaro et al., 2013). This creates unfavorable atmospheric conditions for pollution dispersion and thus worsens surface air pollution. This mechanism was demonstrated clearly in a recent modeling study by Ding et al. (2016). They showed that the aerosol-PBL feedback tends to increase lower PBL pollution and decrease upper PBL pollution.”

2) A decrease of AOD at an altitude about 1km might also been influenced by cloud or mountain fog, in which the in-cloud removal/deposition could also cause a decreased upper altitude negative trend. How did the model deal with the cloud cover issue under high cloud cover condition? Did the authors exclude the days with thick cloud while categorizing days into relatively clean, moderate pollution, and severe pollution scenarios? It will be better to clarify these points in the paper.

As pointed out in the comments, the influence of cloud and mountain fog may result

C2

in an incorrect AOD trend at altitudes above 1000 m. The focus of our work is the aerosol trend and the aerosol-PBL feedback under clear-sky conditions, so the first step is to discriminate between clear and cloudy/foggy conditions. The cloud screening procedures used are added to Section 2 of the revised manuscript:

“A threshold of 90% in relative humidity (RH) is widely used to distinguish between haze (RH < 90%) and fog (RH > 90%) in visibility datasets (Chen and Wang, 2015). However, Ding and Liu (2014) suggested that a value of ~82% may be more suitable for differentiating between haze and fog over China. We use an intermediate value of 85% in our study. For AOD and aerosol extinction profile retrievals from the MFRSR and the MPL, the automated cloud identification algorithm proposed by Alexandrov et al. (2004) was used to screen out cloud-contaminated data. Cloud-free AOD retrievals from the MFRSR are subsequently used to constrain MPL-derived aerosol extinction coefficient profiles according to Welton et al. (2000). It is important to assure that there are no clouds along the pathway of the MPL laser beam when obtaining vertically-integrated aerosol extinction coefficients from the MPL. The column-integrated AOD from the MPL and the AOD retrieved from the MFRSR should be consistent.”

Following this procedure, cloudy measurements were filtered out and the rest of the measurements were categorized according to pollution level: relatively clean, moderately polluted, and severely polluted. Atmospheric radiative heating rates under cloud-free conditions were then simulated.

3) The overall structure of the presentation could be a little bit changed. For example, Fig. 1-5 present results from Guangzhou Plain except Fig. 3, which shows results in the entire China (similar to Fig. 8), and was discussed in the second paragraph of Sec.3.1. How about discussing the Guangzhou Plain results in the first half of the main results part and the results for entire or different regions of China in the latter half? I think it will improve the readability. For Fig. 3 and Fig. 8, the region definition (i.e. range of longitude and latitude) of data for the plot should be included.

C3

We appreciate your suggestions. Figure 2b and Fig. 3 in the original manuscript in Section 3.1 are presented to show that the visibility trends seen in Fig. 2a are reliable and not the result of an artifact due to the influence of clouds or fog. Figure 3 in the original manuscript is also referred to in Section 3.4 to confirm that the trend in the column-integrated AOD is much weaker than that of surface visibility. Figure 8 in the original manuscript is mainly used to show the distinct aerosol-PBL feedback induced by different light-absorbing properties of aerosols. Since the SSA in many parts of China is moderately low (~0.90), similar to the GZP, Figs. 2–7 in the original manuscript are concerned with the main thrust of the study, namely aerosol-PBL interactions due to aerosol absorption. Therefore, we would like to keep the current structure of the paper.

The regions of study shown in Figs. 3 and 8 in the original manuscript are given in Fig. 1 and Fig. 2, respectively.

4) In terms of the calculation of heating rate, it highly depends on light-absorbing property of aerosols. Thus the SSA input data is vital, which ought to be provided in the main text. Additionally, the aerosol-boundary layer feedback play more important role in winter extreme pollution event. How about results during winter?

a) SSA values

SSA is indeed a key variable in determining the sign of the aerosol radiative forcing as well as the magnitude of the heating rate induced by aerosols. In our study, the values of SSA (i.e., 0.84 and 0.80 at 470 and 660 nm, respectively) are taken directly from Lee et al. (2007). In addition, two years of visibility data from surface meteorological observations and BC concentrations measured by an aethalometer (Model AE-31) at the Xi'an site (108.97°E, 34.43°N) are used to evaluate the SSA reported by Lee et al. (2007). According to Xia et al. (2015), visibility measurements are converted to extinction coefficients (in km⁻¹) using the following relationship: $3.912/\text{visibility}$. Absorption coefficients at 532 nm (in km⁻¹) are calculated as $(8.28 \times \text{MBC} + 2.23)/1000$, where MBC

C4

is the BC concentration measured by the AE-31 at 880 nm in units of $\mu\text{g}\cdot\text{m}^{-3}$ (Wu et al., 2009). Using the aforementioned aerosol absorption coefficients from the AE-31 and the aerosol extinction coefficients from visibility data, the corresponding SSA values at 532 nm over the GZP for the years 2011 and 2012 were calculated. The seasonal mean summertime SSA at Xi'an in 2011 and 2012 is 0.79 and 0.83, respectively. The values in winter are 0.76 and 0.77, respectively. The observation-based results in summer generally concur with those from the study of Lee et al. (2007).

b) Wintertime results

As shown in Fig. 3, the profile of AOD trends at different altitudes in winter is similar to that in summer (Fig.3a in the original manuscript). The major difference between the two is that the transition from negative to positive values in AOD trends takes place at a lower altitude. This is because the PBL height is generally lower in winter than in summer. Moreover, the transition zone in the long-term trends in surface visibility over the GZP shows a downward shift as well (not shown here). This finding attests to the notion that the aerosol-PBL feedback plays a more important role in winter. However, unlike the results shown in Fig. 5a and 5b in the original manuscript, the aerosol extinction coefficients above 1500 m during extreme pollution episodes in winter are larger than those during moderate pollution episodes based on MPL retrievals (Fig. 4). This is probably because the portion of AOD in the blind zone of the MPL (0–270 m) in winter is not negligible since pollution is constrained to a much shallower atmospheric layer in winter and cannot be properly removed from the MFRSR-derived AOD, which is used to constrain the aerosol extinction coefficient profile. In other words, the portion of AOD in the lowest 270 m was artificially added to that above 270 m. The magnitude of that portion of AOD is highest during extreme pollution episodes in winter. As a result, the aerosol extinction coefficients are significantly overestimated at all altitudes during extreme pollution episodes.

5) Both of MODIS and MISR retrievals display substantial upper-level decline in AOD trends. For the near-surface increasing AOD, MISR shows much smaller change. What

C5

are the causes for these differences?

The smaller AOD trend values from MISR compared to MODIS at low altitudes can be mostly attributed to the difference in the spatial sampling and spatial resolution of the two instruments.

In our study, operational MODIS level 2 aerosol products with a spatial resolution of 10 km at nadir and MISR level 2 aerosol products with a spatial resolution of 17.6 km are used to generate the gridded AOD dataset at every $0.1^\circ \times 0.1^\circ$ latitude/longitude pair and $0.2^\circ \times 0.2^\circ$ latitude/longitude pair over China, respectively.

As shown in Fig. 4 and Fig. 5a and 5b in the original manuscript, the variation in AOD (or aerosol extinction coefficient) with altitude is more dramatic at low altitudes than at high altitudes. As a result, when AOD retrievals are averaged onto grids over undulating areas at different altitudes, the AOD, as well as the AOD trend, within the grid boxes at low altitudes will be smoothed out. To further investigate this, MODIS level 2 aerosol products were averaged onto $0.2^\circ \times 0.2^\circ$ latitude/longitude grids in the same manner as the MISR aerosol products. Comparisons between MODIS AOD trend profiles for different grid sizes (i.e., $0.1^\circ \times 0.1^\circ$ and $0.2^\circ \times 0.2^\circ$) are shown in Fig. 5. There is almost no difference above 500 m. AOD trend values from the gridded data at the $0.2^\circ \times 0.2^\circ$ spatial resolution are much smaller than those at the $0.1^\circ \times 0.1^\circ$ spatial resolution, suggesting that the smoothing effect induced by a lower spatial resolution exists. Although MODIS and MISR AOD data are averaged using the same grid size, AOD trend values from MODIS (blue dots in Fig. 5) at low altitudes are still larger than those from MISR (Fig. 3b in the original manuscript). Zhang and Reid (2010) demonstrated that even if MODIS and MISR AOD retrievals were averaged onto the same $1^\circ \times 1^\circ$ latitude/longitude grid, MISR trends were still half that of the MODIS trends due to the spatial sampling differences of the two instruments.

References

Alexandrov, M. D., Marshak, A., Cairns, B., Lacis, A. A., and Carlson, B. E.: Auto-

C6

mated cloud screening algorithm for MFRSR data, *Geophys. Res. Lett.*, 31, L04118, doi:10.1029/2003GL019105, 2004.

Barbaro, E., Arellano, V. G., Krol, M. C., and Holtslag, A. A.: Impacts of aerosol short-wave radiation absorption on the dynamics of an idealized convective atmospheric boundary layer, *Bound-Lay. Meteorol.*, 148(1), 31–49, doi:10.1007/s10546-013-9800-7, 2013.

Chen, H. P., and Wang, H. J.: Haze days in North China and the associated atmospheric circulations based on daily visibility data from 1960 to 2012, *J. Geophys. Res. Atmos.*, 120, 5895–5909, doi:10.1002/2015jd023225, 2015.

Ding, A. J., Huang, X., Nie, W., Sun, J. N., Kerminen, V. M., Peteja, T., Su, H., Cheng, Y. F., Yang, X. Q., Wang, M. H., Chi, X. G., Wang, J. P., Virkkula A., Guo, W. D., Yuan, J., Wang, S. Y., Zhang, R. J., Wu, Y. F., Song, Y., Zhu, T., Zilitinkevich, S., Kulmala, M., and Fu, C. B.: Enhanced haze pollution by black carbon in megacities in China, *Geophys. Res. Lett.*, 43, 2873–2879, doi:10.1002/2016gl067745, 2016.

Ding, Y. H., and Liu Y. J.: Analysis of long-term variations of fog and haze in China in recent 50 years and their relations with atmospheric humidity, *Sci. China: Earth Sci.*, 57, 36–46, doi:10.1007/s11430-013-4792-1, 2014.

Gonçalves, W. A., Machado, L. A., and Kirstetter P. E.: Influence of biomass aerosol on precipitation over the Central Amazon: an observational study, *Atmos. Chem. Phys.*, 15, 6789–6800, doi:10.5194/acp-15-6789-2015, 2015.

Lee, K. H., Li, Z., Wong, M. S., Xin, J. Y., Wang, Y. S., Hao, W. M., and Zhao, F. S.: Aerosol single scattering albedo estimated across China from a combination of ground and satellite measurements, *J. Geophys. Res. Atmos.*, 112, D22S15, doi:10.1029/2007jd009077, 2007.

Tesfaye, M., Botai, J., Sivakumar, V., and Tsidu, G. M.: Simulation of biomass burning aerosols mass distributions and their direct and semi-direct effects over South

C7

Africa using a regional climate model, *Meteorol. Atmos. Phys.*, 125(3), 177–195, doi:10.1007/s00703-014-0328-2, 2014.

Welton, E. J., Voss, K. J., Gordon, H. R., Maring, H., Smirnov, A., Holben, B., Schmid, B., Livingston, J. M., Russell, P. B., Durkee, P. A., Formenti, P., and Andreae, M. O.: Ground-based lidar measurements of aerosols during ACE-2: instrument description, results, and comparisons with other ground-based and airborne measurements, *Tellus*, 52, 636–651, doi: 10.1034/j.1600-0889.2000.00025.x, 2000.

Wu, D., Mao, J. T., Deng, X. J., Tie, X. X., Zhang, Y. H., Zeng, L. M., Li, F., Tan, H. B., Bi, X. Y., Huang, X. Y., Chen, J. and Deng T.: Black carbon aerosols and their radiative properties in the Pearl River Delta region, *Sci. China - Earth Sci.*, 52(8), 1152–1163, doi:10.1007/s11430-009-0115-y, 2009.

Xia, H. Y., Shentu, G., Shanguan, M. J., Xia, X. X., Jia, X. D., Wang, C., Zhang, J., Pelc, J. S., Fejer, M. M., Zhang, Q., Dou, X. K., and Pan J. W.: Long-range micro-pulse aerosol lidar at 1.5 μm with an upconversion single-photon detector, *Opt. Lett.*, 40(7), 1579–1582, doi:10.1364/OL.40.001579, 2015.

Zhang, J., and Reid, J. S.: A decadal regional and global trend analysis of the aerosol optical depth using a data-assimilation grade over-water MODIS and Level 2 MISR aerosol products, *Atmos. Chem. Phys.*, 10, 10949–10963, doi:10.5194/acp-10-10949-2010, 2010.

Zhang, Y., Fu, R., Yu, H. B., Dickinson, R. E., Juarez, R. N., Chin, M., and Wang, H.: A regional climate model study of how biomass burning aerosol impacts land-atmosphere interactions over the Amazon, *J. Geophys. Res. Atmos.*, 113, d14s15, doi:10.1029/2007jd009449, 2008.

Interactive comment on *Atmos. Chem. Phys. Discuss.*, doi:10.5194/acp-2017-2, 2017.

C8

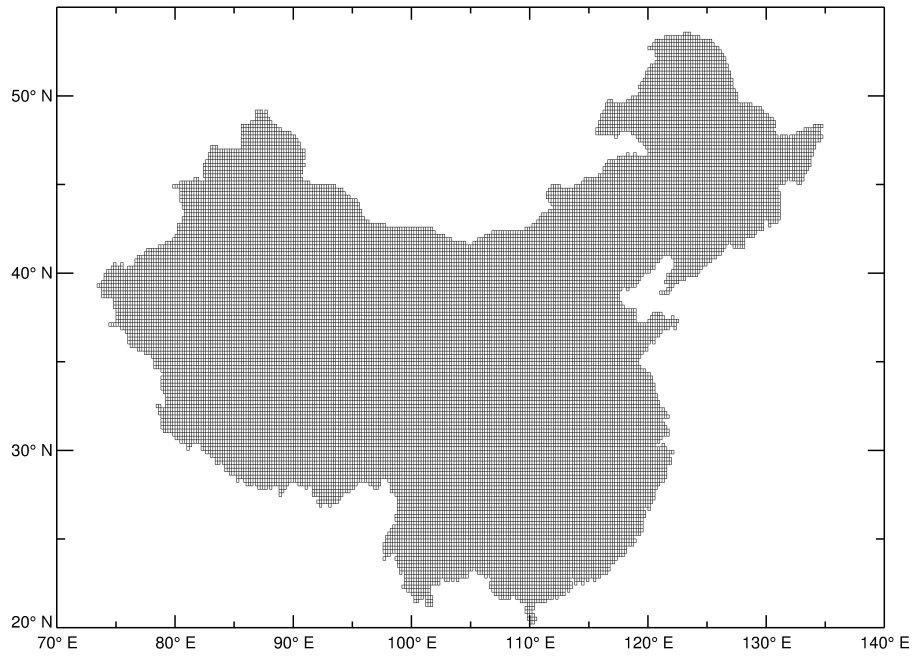


Fig. 1. The region of study in Fig. 3 in the original manuscript.

C9

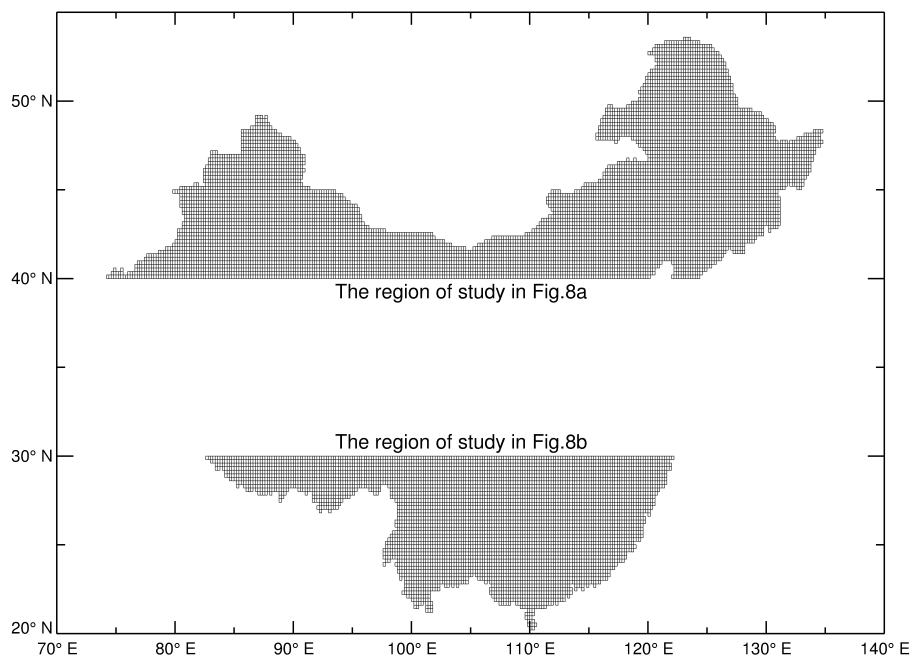


Fig. 2. The regions of study in Fig. 8 in the original manuscript.

C10

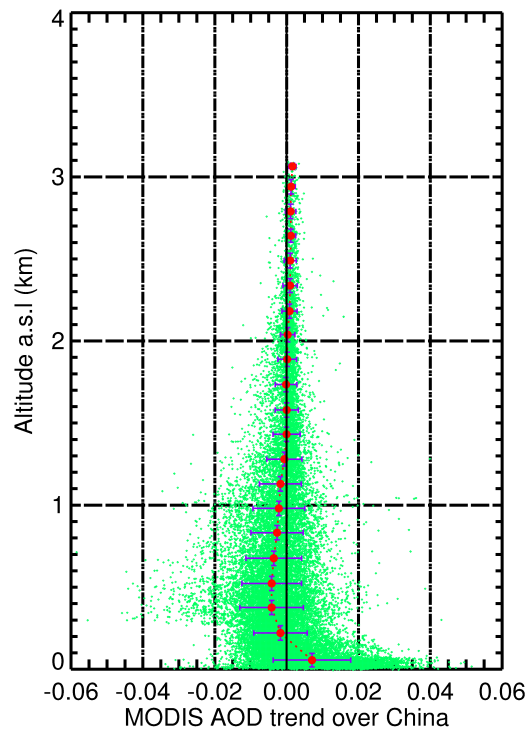


Fig. 3. Vertical profiles of the trend in AOD from MODIS-Aqua from 2002 to 2014 over China. The “a.s.l” in the ordinate labels stands for “above sea level”.

C11

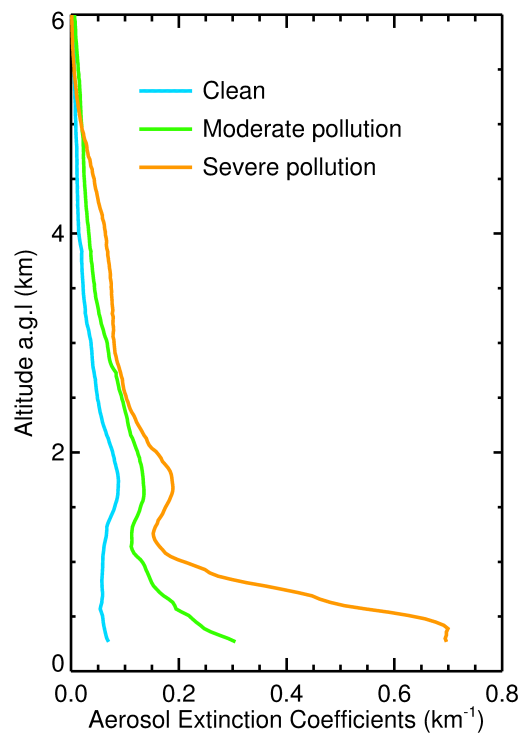


Fig. 4. Mean wintertime aerosol extinction profiles measured by the MPL in 2014 under different pollution level conditions. Profiles representing relatively clean, moderate pollution and severe pollution scen

C12

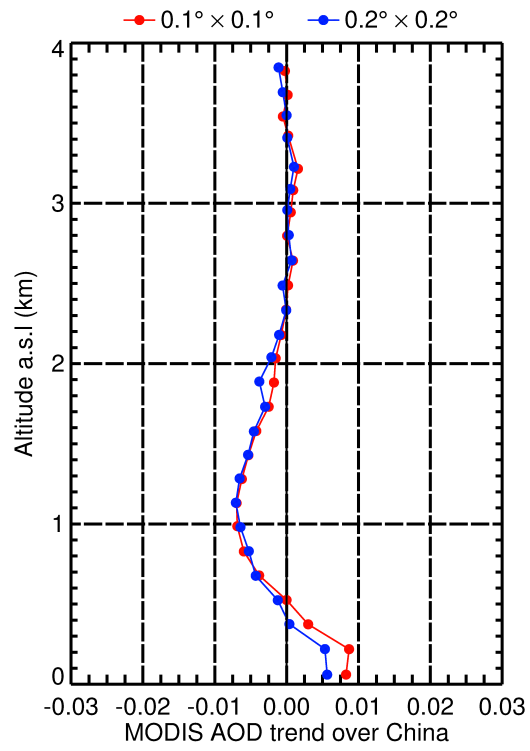


Fig. 5. Vertical profiles of aerosol optical depth (AOD) trends over the entirety of China from gridded MODIS AOD data at $0.1^\circ \times 0.1^\circ$ (red dots and red line) and $0.2^\circ \times 0.2^\circ$ (blue dots and blue line) spatial reso